

A mean field dynamo from negative eddy diffusivity

Ebru Devlen,^{1,2*} Axel Brandenburg^{1,3} and Dhrubaditya Mitra¹

¹*Nordita, KTH Royal Institute of Technology and Stockholm University, Roslagstullsbacken 23, 10691 Stockholm, Sweden*

²*Department of Astronomy & Space Sciences, Faculty of Science, University of Ege, Bornova 35100, Izmir, Turkey*

³*Department of Astronomy, Stockholm University, 10691 Stockholm, Sweden*

Accepted 2013 April 4. Received 2013 April 4; in original form 2012 December 15

ABSTRACT

Using direct numerical simulations, we verify that Roberts-IV flow exhibits dynamo action dominated by horizontally averaged large-scale magnetic field. With the test-field method, we compute the turbulent magnetic diffusivity and find that it is negative and overcomes the molecular diffusivity, thus explaining quantitatively the large-scale dynamo for magnetic Reynolds numbers above ≈ 8 . As expected for a dynamo of this type, but contrary to α -effect dynamos, the two horizontal field components grow independently of each other and have arbitrary amplitude ratios and phase differences. Small length-scales of the mean magnetic field are shown to be stabilized by the turbulent magnetic diffusivity becoming positive at larger wavenumbers. Oscillatory decaying or growing solutions have also been found in certain wavenumber intervals and sufficiently large values of the magnetic Reynolds number. For magnetic Reynolds numbers below ≈ 0.5 , the turbulent magnetic diffusivity is confirmed to be positive, as expected for all incompressible flows. Earlier claims of a dynamo driven by a modified Taylor–Green flow through negative eddy diffusivity could not be confirmed.

Key words: dynamo – magnetic fields – MHD – turbulence.

1 INTRODUCTION

The equations of magnetohydrodynamics (MHD) permit growth of magnetic energy at the expense of kinetic energy. This phenomenon is called the dynamo effect (see e.g. Brandenburg & Subramanian 2005 for a recent review). If the dynamo effect gives rise to a magnetic field whose characteristic length-scale is greater than that of the fluid, we call it a *large-scale* dynamo. Most astrophysical dynamos, including the solar dynamo and the Galactic dynamo, are of this type.

To theoretically describe the large-scale dynamo, one must average the equations of MHD over the small scales to obtain an effective equation for the large-scale magnetic field. This effective equation can be written down by using either mean-field theory (Steenbeck, Krause & Rädler 1966) or multiple-scale expansions (see e.g. Zheligovsky 2011 for a recent review). These equations contain turbulent transport coefficients: the α -effect and turbulent diffusivity. In general, both are tensors whose complexity depends on the symmetries of the problem. Within the formalism of mean-field theory, it is generally a non-trivial task to calculate the turbulent transport coefficients even if we ignore the back-reaction of the magnetic field on the flow, i.e. for kinematic dynamos. For several kinematic problems, the turbulent transport coefficients have been calculated using the test-field method (TFM) of Schrunner et al. (2005, 2007); see

also Brandenburg (2005), Brandenburg et al. (2008a), Brandenburg, Rädler & Schrunner (2008b). Typically, it is found that the α -effect gives rise to the growth of a large-scale magnetic field while the turbulent diffusivity contributes to decay by effectively enhancing the molecular magnetic diffusivity. However, multiscale methods have shown that for certain flows the α -effect can be zero, but the eddy diffusivity, i.e. the sum of turbulent and molecular diffusivity, may turn out to be negative (see e.g. Lanotte et al. 1999; Zheligovsky, Podvigina & Frisch 2001). In that case, such flows may act as large-scale dynamos. However, we are not aware of direct numerical simulations (DNS) that demonstrate that those flows really do produce mean magnetic fields and that this is caused by negative eddy diffusivity.

In a remarkable paper, Roberts (1972) shows that the multiple-scale versions of two-dimensional spatially periodic motions can give growing magnetic fields for magnetic diffusivities below a critical value. He studies four different periodic flow patterns. We are here especially interested in flow IV (in the following referred to as Roberts-IV flow) because, although this flow yields exponentially growing solutions in time (see his fig. 10), he finds all components of the α tensor to be zero. Roberts (1972) also notes that his results are relevant to turbulent dynamos with positive turbulent diffusivity, but the possibility of negative turbulent diffusivity is not discussed explicitly. In this paper, we first verify, using DNS, that for a particular flow (Roberts 1972), namely the Roberts-IV flow, it is possible to drive a kinematic large-scale dynamo, although the α -effect and the planar-averaged kinetic helicity are indeed zero. Next, by using

*E-mail: devlen@nordita.org

the TFM, we show that such a dynamo can be accurately described by zero α -effect but negative turbulent diffusivity which dominates over the molecular one. (In the context of laminar flows, the expression *turbulent* diffusivity is not optimal, and refers simply to a diffusion-like coefficient in the averaged equations.)

Finally, we turn to the Taylor–Green (TG) and the modified TG flows for which negative eddy diffusivity dynamos have been claimed previously (Lanotte et al. 1999). Again, these flows have no net helicity. Although dynamo action was found in several cases, no large-scale magnetic field was found in DNS of these flows. Furthermore, the α -effect turns out to be zero, but the eddy diffusivity remains positive. This flow does therefore not appear to be an example of a negative eddy diffusivity dynamo.

2 THE ROBERTS-IV FLOW

In connection with understanding the geodynamo, Tilgner (2004) studied in some detail the Roberts-IV flow. We follow here Tilgner’s definition of the flow:

$$\mathbf{U} = u_0 \begin{Bmatrix} \sqrt{2/f} \sin k_0 x \cos k_0 y \\ -\sqrt{2/f} \cos k_0 x \sin k_0 y \\ \sqrt{f} \sin k_0 x \end{Bmatrix}, \quad (1)$$

where u_0 characterizes the amplitude of the flow. It is solenoidal and its vorticity, $\mathbf{W} = \nabla \times \mathbf{U}$, is given by

$$\mathbf{W} = u_0 \begin{Bmatrix} 0 \\ -\sqrt{f} k_0 \cos k_0 x \\ 2\sqrt{2/f} k_0 \sin k_0 x \sin k_0 y \end{Bmatrix}. \quad (2)$$

Here, the parameter f determines the relative importance of vertical to horizontal motions. The kinetic helicity density, $\mathbf{W} \cdot \mathbf{U}$, is given by

$$\mathbf{W} \cdot \mathbf{U} = \sqrt{2} u_0^2 k_0 (1 + \sin^2 k_0 x) \sin k_0 y \quad (3)$$

and is independent of f . Tilgner (2004) showed that in spite of the horizontally averaged kinetic helicity density, $\overline{\mathbf{W} \cdot \mathbf{U}}$, being zero, the Roberts-IV flow gives rise to dynamo action. In other words, it leads to growing solutions of the induction equation,

$$\frac{\partial \mathbf{B}}{\partial t} = \nabla \times (\mathbf{U} \times \mathbf{B} - \eta \mathbf{J}), \quad (4)$$

where η is the microphysical (molecular) magnetic diffusivity, \mathbf{B} is the magnetic field, $\mathbf{J} = \nabla \times \mathbf{B}$ is the current density, and we have chosen our units such that the vacuum permeability is unity.

Note, however, that Tilgner (2004) described the dynamo to be a small-scale one, i.e. the characteristic length-scales of the magnetic field is of the same order as $1/k_0$. In the following, we obtain solutions to equation (4) via DNS using the PENCIL CODE.¹ We do not evolve the flow, hence we study kinematic dynamo solutions.

As an example of the resulting magnetic field, we show in Fig. 1 the three components of the magnetic field at the periphery of the computational domain. It is remarkable that the resulting magnetic field has a large-scale component that survives xy averaging (denoted by overbars), i.e. $\overline{\mathbf{B}} = \overline{\mathbf{B}}(z, t)$ is non-vanishing; see Fig. 2, where we show examples of the resulting mean field obtained by averaging the solution of the DNS. In other words, we have here

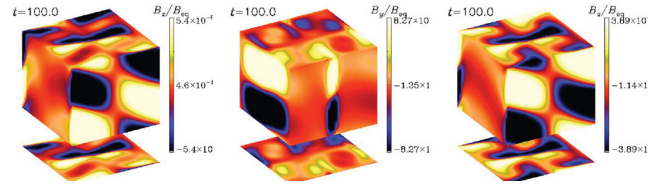


Figure 1. Three components of the magnetic field on the periphery of the computational domain for $R_m = 20$, $f = 1$, and domain size $L_x = L_y = L_z = 2\pi/k_0$.

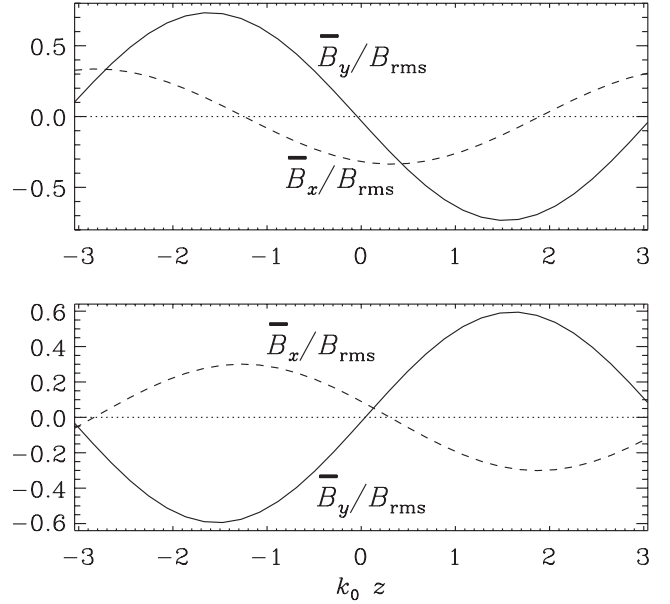


Figure 2. Examples of runs with two different initial conditions (upper and lower panels) showing the x and y components of the mean field (normalized by the rms value of the total field \mathbf{B}) versus z , obtained from the DNS for $f = 1$, $L_x = L_y = L_z = 2\pi/k_0$ and $\eta = 0.05 u_0/k_0$, corresponding to $R_m = 20$.

an example of a mean-field dynamo with $\overline{\mathbf{B}}$ being a solution of the horizontally averaged induction equation,

$$\frac{\partial \overline{\mathbf{B}}}{\partial t} = \nabla \times (\overline{\mathbf{U}} \times \overline{\mathbf{B}} + \overline{\mathcal{E}} - \eta \overline{\mathbf{J}}), \quad (5)$$

where $\overline{\mathcal{E}} = \overline{\mathbf{u} \times \mathbf{b}}$ is the mean electromotive force resulting from correlations of residual velocity and magnetic fields, $\mathbf{u} = \mathbf{U} - \overline{\mathbf{U}}$ and $\mathbf{b} = \mathbf{B} - \overline{\mathbf{B}}$, respectively. (Note that here $\overline{\mathbf{U}} = 0$.) Empirically, we find that the horizontally averaged solutions of equation (4) are of the form

$$\overline{\mathbf{B}}(z, t) = \begin{Bmatrix} B_{0x} \cos(kz + \phi_x) \\ B_{0y} \cos(kz + \phi_y) \\ 0 \end{Bmatrix} e^{\lambda t}, \quad (6)$$

where B_{0x} , B_{0y} , ϕ_x and ϕ_y are arbitrary constants, i.e. the x and y components of the magnetic field evolve independently of each other and they have arbitrary phase shifts, depending just on the properties of the initial conditions; see Fig. 2 for an example. The same result can be inferred from equation 7.3 of Roberts (1972). Solutions of equation (5) can be obtained by mean-field simulations which requires a closed expression for $\overline{\mathcal{E}}$ in terms of $\overline{\mathbf{B}}$. This will be discussed in the following.

As pointed out by Tilgner (2004), the Roberts-IV flow has no α -effect. As this is a laminar flow, driving a dynamo via fluctuations

¹ <http://pencil-code.googlecode.com/>

of the α -effect (Mitra & Brandenburg 2012) is also not possible. This suggests that the observed mean field might be produced by a negative eddy diffusivity (Lanotte et al. 1999; Zheligovsky et al. 2001). To investigate such a possibility, we now apply the TFM to calculate the turbulent transport coefficients of the Roberts-IV flow.

As is long recognized (Rädler 1976), the connection between $\bar{\mathcal{E}}$ and $\bar{\mathbf{B}}$ is a non-local one that is described by a convolution of the form

$$\bar{\mathcal{E}}_i = \hat{\alpha}_{ij} \circ \bar{B}_j - \hat{\eta}_{ij} \circ \bar{J}_j, \quad (7)$$

where ‘ \circ ’ denotes a convolution in space and time, i.e.

$$\hat{\eta}_{ij} \circ \bar{J}_j = \iint \hat{\eta}_{ij}(z - z', t - t') \bar{J}_j(z', t') dz' dt', \quad (8)$$

and likewise for $\hat{\alpha}_{ij} \circ \bar{B}_j$, but this term is vanishing for the Roberts-IV flow (Tilgner 2004). The hats on $\hat{\alpha}_{ij}$ and $\hat{\eta}_{ij}$ indicate that the corresponding quantities are integral kernels.

We emphasize that in equation (7) we have made use of the fact that the only non-vanishing derivatives of a horizontally averaged mean field are $\partial \bar{B}_x / \partial z$ and $\partial \bar{B}_y / \partial z$, which be expressed in terms of components of $\bar{\mathbf{J}}$, so the corresponding turbulent diffusivity tensor is just of rank 2, not, as in the general case of rank 3 (Krause & Rädler 1980).

In the TFM, the kernel formulation above is most naturally considered in Fourier space with

$$\tilde{\mathcal{E}}(k, \omega) = \tilde{\alpha}_{ij}(k, \omega) \tilde{B}_j(k, \omega) - \tilde{\eta}_{ij}(k, \omega) \tilde{J}_j(k, \omega), \quad (9)$$

where tildes denote appropriately normalized Fourier transforms of the corresponding mean-field quantities (Brandenburg et al. 2008b; Hubbard & Brandenburg 2009). The usual α -effect and turbulent diffusivity emerge in the limits $k \rightarrow 0$ and $\omega \rightarrow 0$ for the respective quantities. Hereafter, we drop the tildes even when the k and ω arguments are indicated to be non-vanishing.

In the following, we consider a three-dimensional domain of size $L_x \times L_y \times L_z$. For most cases we choose cubic domains, i.e. $L_x = L_y = L_z = 2\pi/k_0$. We are primarily interested in the case of harmonic solutions of equation (5) with given vertical wavenumber k of a magnetic field that is growing or decaying exponentially proportional to $e^{\lambda t}$. So we are interested in the case $\omega = i\lambda$. As an approximation, we begin by considering the case $\omega = 0$, i.e. we ignore the so-called memory effect; see Hubbard & Brandenburg (2009) for illustrating the departure in the case of the standard Roberts flow with helicity (also known as the Roberts-I flow).

3 RESULTS

In the following, we use the TFM, as described in Brandenburg et al. (2008b) and Hubbard & Brandenburg (2009).

3.1 Sign change of eddy diffusivity

As we have already mentioned, all components of $\alpha_{ij}(k, \omega)$ vanish for the Roberts-IV flow. Moreover, $\eta_{ij}(k, \omega)$ is isotropic, i.e. we can write $\eta_{ij} = \eta_t \delta_{ij}$. In practice, we compute $\eta_t = (\eta_{11} + \eta_{22})/2$ and find that $\epsilon_\eta = (\eta_{11} - \eta_{22})/2$ vanishes to numerical accuracy. A priori the fact that $\eta_{ij}(k, \omega)$ is isotropic is surprising because the z component of the flow is not isotropic. This is also confirmed by analytical calculation using the second-order correlation approximation (SOCA), as shown by Rädler (private communication). Indeed, this isotropy is broken once we allow for averages that depend on y and z , but with that definition of averages, α is no longer zero. This leads to

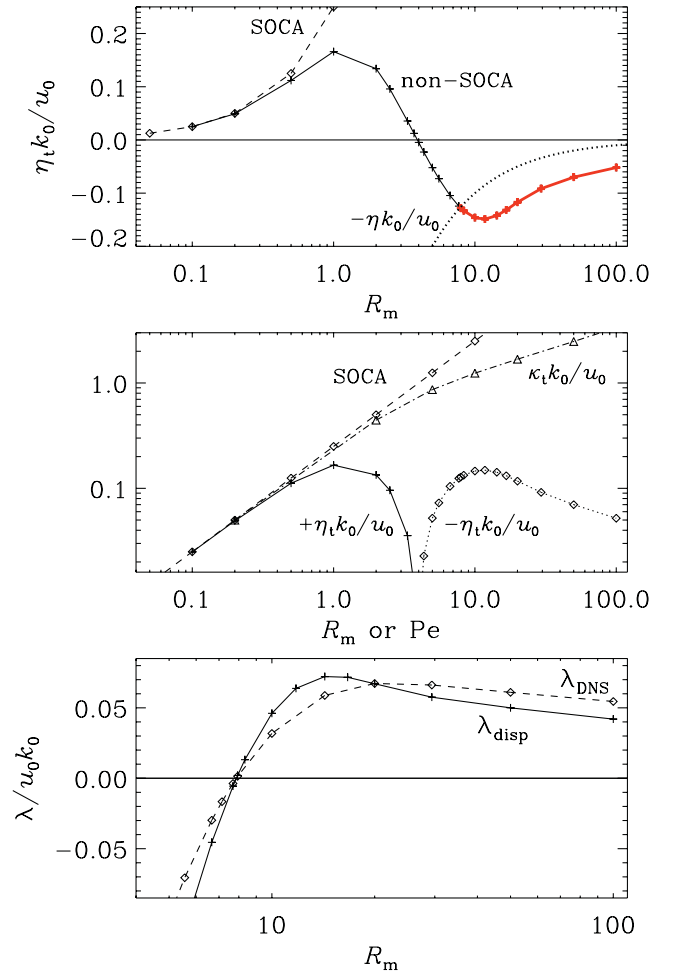


Figure 3. Turbulent magnetic diffusivity, η_t (top and middle panels), and growth rates λ_{disp} and λ_{DNS} versus R_m for $f = 1$ and $k = k_0$. In the first two panels, the dashed lines give the SOCA result, $\eta_t k_0 / u_0 = R_m / 4$. In the first panel, the intersection between η_t and $-\eta$ (dotted line) marks the onset of dynamo action at $R_m \approx 8$. (The section for $R_m > 8$ is marked in red/thick.) The double-logarithmic representation in the middle panel allows one to see that the linear SOCA dependence is obeyed for $R_m \lesssim 0.5$. Note also that the turbulent passive scalar diffusivity, κ_t , remains positive (triangles and dash-dotted line).

other interesting interpretations regarding negative eddy diffusivity dynamos that will be investigated in a future publication.

The resulting values of $\eta_t(k_0, 0)$ are shown in Fig. 3 as a function of magnetic Reynolds number,

$$R_m = u_0 / \eta k_0. \quad (10)$$

For comparison with earlier work involving turbulent flows, we note that this definition of R_m is close to a definition in terms of the rms velocity of the flow (for $f = 1$ we have $u_{\text{rms}} \approx 1.225 u_0$) and the wavenumber of the energy-carrying eddies k_f , i.e. $u_{\text{rms}} / \eta k_f$. If we approximate $k_f \approx w_{\text{rms}} / u_{\text{rms}}$, where w_{rms} is the rms value of the fluctuating part of the vorticity, then we have $k_f \approx 1.29 k_0$. Therefore, we have $u_{\text{rms}} / \eta k_f \approx 0.95 R_m$, which is close to R_m .

As is common to many turbulent transport coefficients (Brandenburg, Rädler & Schrunner 2008b; Sur, Brandenburg & Subramanian 2008), η_t grows linearly with R_m for $R_m \lesssim 0.5$; see the middle panel of Fig. 3. More importantly, η_t is positive, which is to be expected based on a calculation for incompressible flows using SOCA, which is valid for $R_m \ll 1$. To show this, one uses the fact that the Fourier

transform of the velocity correlation tensor is positive semidefinite. We note in passing that this is not true for potential flows, for which the turbulent diffusion tensor is negative semidefinite for $R_m \ll 1$; see Rädler et al. (2011) for a recent demonstration using the TFM.

Returning now to the Roberts-IV flow, which is indeed incompressible, we show in Fig. 3 that η_t changes sign from positive to negative at $R_m \approx 4$. This is clearly a result that cannot be recovered by SOCA. A corresponding calculation for the turbulent passive scalar diffusivity, κ_t (e.g. Brandenburg, Svedin & Vasil 2009), shows that its value remains positive and close to the SOCA value for small Péclet numbers, $Pe = u_0/\kappa k_0$, where κ is the microphysical (molecular) passive scalar diffusivity.

Our TFM results show that, for $R_m \approx 8$, the total magnetic diffusivity, $\eta + \eta_t(k, 0)$ becomes negative, i.e. dynamo action by the negative magnetic diffusivity effect is possible. The critical value of R_m agrees with that found above through DNS. The growth rate of the dynamo is given in implicit form as a solution of the equation

$$\lambda(k) = -[\eta + \eta_t(k, i\lambda)]k^2 \quad (11)$$

for $k = k_0$. However, it is common to approximate $\eta_t(k_0, \omega)$ by $\eta_t(k_0, 0)$, and we refer to the corresponding solution as

$$\lambda(k) \approx \lambda_{\text{disp}}(k) = -[\eta + \eta_t(k, 0)]k^2, \quad (12)$$

which is shown in the third panel of Fig. 3 and compared with the growth rate λ_{DNS} obtained by solving equation (4) through DNS. The agreement between λ_{disp} and λ_{DNS} is moderate and reminiscent of what has been found earlier (Hubbard & Brandenburg 2009). By using test fields that grow exponentially at a rate that is equal to the expected growth rate, $\lambda = \lambda_{\text{DNS}}$, we find for $\eta = 0.020 u_0/k_0$ (corresponding to $R_m \approx 50$), the value $\eta_t(k_0, i\lambda_{\text{DNS}}) = -0.081 u_0/k_0$ with $\lambda_{\text{DNS}} = 0.061 u_0 k_0$, instead of the value $\lambda = -0.070 u_0 k_0$ obtained with $\eta_t(k_0, 0) = 0$. Thus, perfect agreement between DNS and TFM is obtained once the memory effect included.

3.2 Dependence on f

Let us now discuss the dependence on the parameter f , which characterizes the relative importance of vertical to horizontal motions. We consider here the case of $R_m = 20$ and $k = k_0$. The results are shown in Fig. 4. The negative turbulent diffusivity dynamo is found

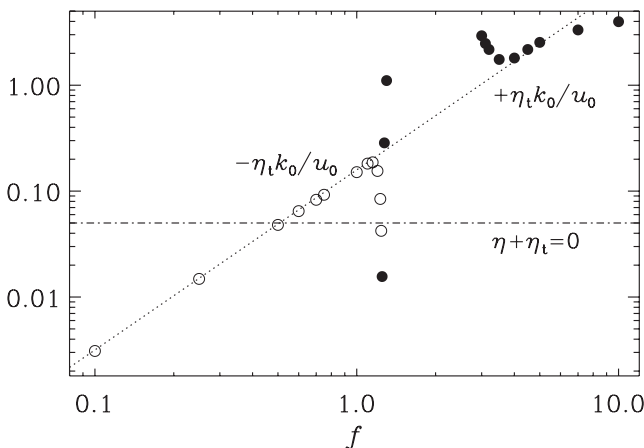


Figure 4. Dependence of turbulent diffusivity on f for $R_m = 20$ and $k = k_0$. Negative (positive) values of η_t are indicated with open (filled) symbols, and the horizontal dash-dotted line indicates the region above which there is dynamo action, because $\eta + \eta_t < 0$. The dotted line has a slope of 1.7 and is shown for orientation.

to be operating in the range $0.6 \leq f \leq 1.23$, i.e. when the vertical turbulent diffusivity is not much larger than the horizontal.

As indicated by the dotted line in Fig. 4, both for small and for large values of f , there is an approximate power-law dependence with $|\eta_t| \sim f^{1.7}$. However, in the range $1.3 < f < 3$ the TFM diverges and is unable to deliver useful results. Diverging results of the TFM are common and related to unstable eigenvalues of the associated homogeneous system of equations solved in the TFM. Usually, this problem can be avoided by restricting the analysis of the test problems to limited time intervals (Hubbard et al. 2009; Rheinhardt & Brandenburg 2010), but in the present case the solutions were diverging immediately.

3.3 Scale dependence and memory effect

Owing to the k^2 factor in equations (11) and (12), one might expect dynamos driven by negative eddy diffusivity to grow faster at larger values of k (smaller scales), unless $\eta + \eta_t$ changes and becomes positive at larger k . To study this, we now employ test fields with $k \neq k_0$. In Fig. 5, we show the k dependence of $\eta_t(k, 0)$. It turns out that $\eta_t(k, 0)$ is approximately constant for $k \leq k_* \approx 1.125 k_0$, and positive with an approximate dependence

$$\eta_t(k, 0) \approx \frac{0.31 u_0/k_0}{[(k - k_\infty)/k_0]^{0.7}} \quad \text{for } k > k_\infty, \quad (13)$$

where $k_\infty \approx 2.25 k_0$. In the range $k_* < k < k_\infty$, we have two data points in Fig. 5 that clearly deviate from the description above. In addition, there are several other values of k in this range where the TFM again diverges and is unable to deliver useful results.

To illuminate the problem of intermediate k values further, we now use DNS to compute the growth rate as a function of the domain size L_z , decreased according to $L_z = 2\pi/k$. The result is shown in Fig. 6. It turns out that $\lambda (= \lambda_{\text{DNS}})$ has a maximum at $k/k_0 \approx 1.04$ (corresponding to $L_z k_0 \approx 6$). Thus, large-scale separation, as assumed in some analytic studies (Lanotte et al. 1999), is neither needed nor necessarily helpful for the operation of this negative eddy diffusivity dynamo. Furthermore, for $k/k_0 \approx 1.23$ (corresponding to $L_z k_0 \leq 5.1$), no dynamo is possible and the field decays in an oscillatory fashion. The oscillation frequency ω grows sharply as k increases further; see the dotted line in Fig. 6. However, when the dynamo is excited, it is non-oscillatory. While Roberts (1972)

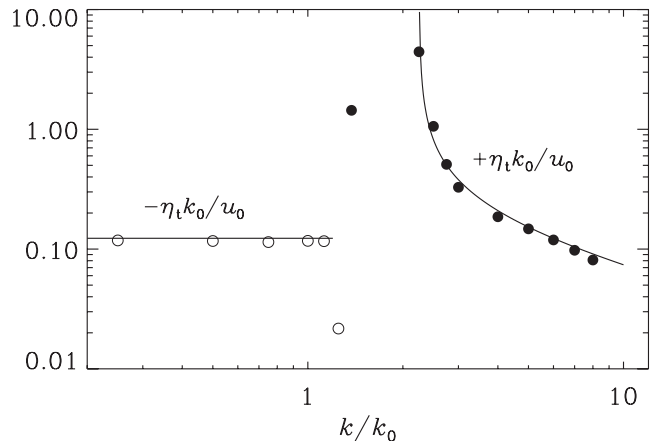


Figure 5. Wavenumber dependence of turbulent diffusivity for $R_m = 20$ and $f = 1$. Note that dynamo action is only possible for $k/k_0 \leq 1.25$, i.e. when η_t is negative.

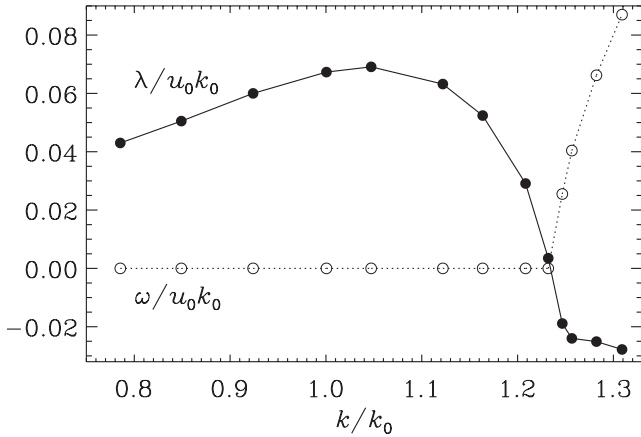


Figure 6. Dependence of the growth rate λ and the oscillation frequency ω on k (using a correspondingly adjusted domain size $L_z = 2\pi/k$) for $R_m = 20$ and $f = 1$. In all cases with $\lambda > 0$, we have $\omega = 0$.

also finds non-oscillatory behaviour in the dynamo cases, he finds non-oscillatory decaying solutions, but at smaller R_m .

At the level of a simplistic description of a mean-field dynamo with negative eddy diffusivity, the occurrence of oscillations in the subcritical case must be surprising. However, this puzzle is easily resolved by reinstating the ω dependence of $\eta_t(k, \omega)$ in equation (9). This corresponds to the memory effect, i.e. the dependence of \mathcal{E} on the mean magnetic field at past times.

A simple prescription of the memory effect would be to assume that η_t is proportional to the analytic function $1/(1 - i\omega\tau)$, where τ is a characteristic time-scale of the flow. Following Hubbard & Brandenburg (2009), we replace $-i\omega$ by the Laplace variable s and assume that the growth rate is equal to $\text{Re } s$ and the frequency is $\omega = -\text{Im } s$. This leads to the dispersion relation

$$s\tau = -\tau\eta_t k^2 / (1 + s\tau) - \tau\eta_t k^2. \quad (14)$$

Solving this quadratic equation for $s\tau$, we find

$$s_{\pm}\tau = -\frac{1}{2}(1 + n) \pm \frac{1}{2}\sqrt{(1 - n)^2 - 4n_t}, \quad (15)$$

where $n = \tau\eta_t k^2$ and $n_t = \tau\eta_t k^2$ have been introduced. Here, only the upper sign corresponds to physically realizable solutions that can grow for negative eddy diffusivity, $\eta_t + \eta < 0$. In that case, $s\tau$ is real, but complex for positive turbulent diffusivity, $n_t > 0$. This explains qualitatively the occurrence of oscillatory decay, except that this formula would also predict a narrow n_t interval of non-oscillatory decay which is not seen in the data.

The actual form of $\eta_t(k, \omega)$ near onset at $k/k_0 \approx 1.23$ is of course more complicated. The result, obtained using the method described by Hubbard & Brandenburg (2009), is shown in Fig. 7. For $\omega/u_0k_0 > 0.5$, a reasonable fit to the data is given by

$$\eta_t(k, \omega) \approx \frac{u_0 k_0}{[1 + b(\omega/u_0k_0)^4]^2} \sum_{n=0}^4 a_n \left(-\frac{i\omega}{u_0k_0} \right)^n, \quad (16)$$

with empirical coefficients $a_0 = -0.055$, $a_1 = 0.5$, $a_2 = -0.35$, $a_3 = 0.2$, $a_4 = -0.02$ and $b = 0.031$. On the other hand, for small departures from the stationary state, $\omega/u_0k_0 \ll 0.5$, a good approximation is $\eta_t = -0.055 u_0 k_0 / (1 - i\omega\tau)$ with $\tau \approx 2/u_0k_0$, confirming thus our initial ansatz. For larger values of k , when $\text{Re } \eta_t$ becomes positive, there is a rapid increase of τ , which explains why the aforementioned interval with non-oscillatory decay is absent.

In analogy with α -effect mean-field dynamos, where the wavenumber of the fastest growing mode increases with dynamo

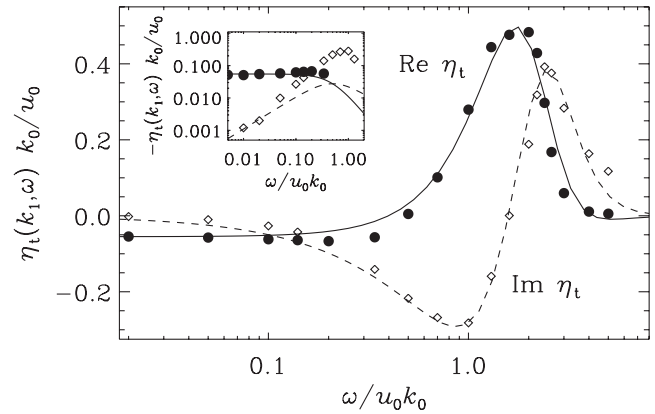


Figure 7. Dependence of real and imaginary parts of $\bar{\eta}_t$ on ω for the case $k/k_0 \approx 1.23$, $R_m = 20$ and $f = 1$ compared with the empirical fit given by equation (16). Real (imaginary) parts are indicated by filled (open) symbols and solid (dashed) lines. The inset shows that for $\omega/u_0k_0 < 0.1$, the data are well described by $\eta_t = -0.055 u_0 k_0 / (1 - i\omega\tau)$ with $\tau \approx 2/u_0k_0$.

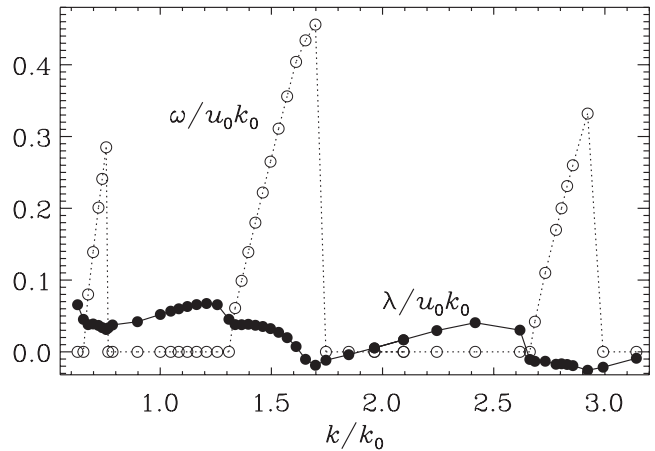


Figure 8. Similar to Fig. 6, but for $R_m = 100$. Note the existence of growing oscillatory solutions in the ranges $0.6 \lesssim k/k_0 \lesssim 0.8$ and $1.3 \lesssim k/k_0 \lesssim 1.7$.

number, one may ask whether this is also true of the negative magnetic diffusivity dynamo. In Fig. 8, we show the result for $R_m = 100$. It turns out that the wavenumber of the fastest growing mode increases slightly (from $k/k_0 \approx 1.04$ at $R_m = 20$ to ≈ 1.21 at $R_m = 100$). For larger values of k , the solutions become again oscillatory, but, in contrast to the case of smaller values of R_m , the modes are now not decaying. Looking at Fig. 8, it becomes clear that the explanation in terms of the simplest form of the memory effect no longer applies, and that a more detailed dependence on ω would need to be considered.

4 MODIFIED TAYLOR-GREEN FLOWS

While the possibility of a dynamo driven by negative eddy diffusivity has not been previously quantified for the Roberts-IV flow, it was discussed in some detail by Lanotte et al. (1999) for the TG flow,

$$\mathbf{U}_{\text{TG}} = u_0 \begin{Bmatrix} \sin k_0 x \cos k_0 y \cos k_0 z \\ -\cos k_0 x \sin k_0 y \cos k_0 z \\ 0 \end{Bmatrix}, \quad (17)$$

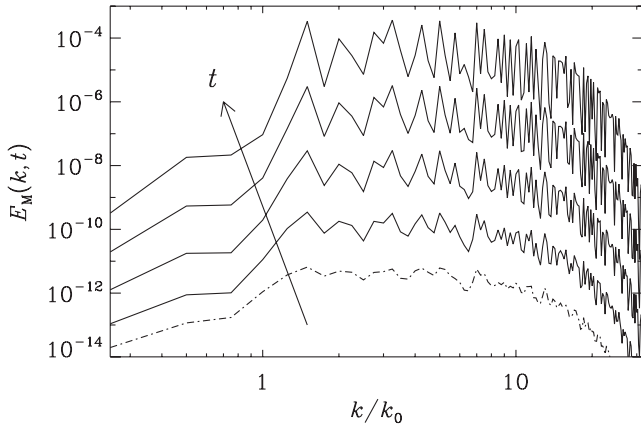


Figure 9. Magnetic power spectra of DNS for the TG flow with $A = 1$ and $B = 0$ in a domain of size $L_x = L_y = L_z = 8\pi/k_0$ using 256^3 mesh points and $\eta = 0.02 u_0/k_0$ at different times during the exponential growth phase of the dynamo. The earliest time is shown as a dash-dotted line.

and the modified TG flow, $U_{\text{TG}} + AU_A + BU_B$, where A and B denote the amplitudes of additional contributions proportional to

$$U_A = u_0 \begin{Bmatrix} \sin 2k_0 x \cos 2k_0 z \\ \sin 2k_0 y \cos 2k_0 z \\ -(\cos 2k_0 x + \cos 2k_0 y) \sin 2k_0 z \end{Bmatrix}$$

and

$$U_B = u_0 \begin{Bmatrix} (\sin k_0 x \cos 3k_0 y + \frac{5}{13} \sin 3k_0 x \cos k_0 y) \cos k_0 z \\ -(\cos 3k_0 x \sin k_0 y + \frac{5}{13} \cos k_0 x \sin 3k_0 y) \cos k_0 z \\ \frac{2}{13} (\cos k_0 x \cos 3k_0 y - \cos 3k_0 x \cos k_0 y) \sin k_0 z \end{Bmatrix},$$

respectively.

We have performed kinematic DNS with this flow and we indeed find dynamo action. We carry out calculations for $\eta = 0.02 u_0/k_0$, which corresponds to the case where the dynamo is mildly supercritical. We consider the following three cases: (a) a cube of size $L_x = L_y = L_z = 2\pi/k_0$, using 128^3 meshpoints; (b) a cuboid with $L_z = 4L_x$ and $L_y = L_x = 2\pi/k_0$, using $128^2 \times 512$ meshpoints and (c) a cuboid with $L_x = L_y = 4L_z$ and $L_z = 2\pi/k_0$. In all these cases, the large-scale field obtained by averaging over the xy plane decays as a function of time, i.e. *no* large-scale dynamo is obtained with this average. However, there still remains, in principle, the possibility of a large-scale field developing that is zero under xy averaging but is non-zero under another averaging procedure, e.g. Fourier filtering. But even this possibility is ruled out because we observe no growth of a large-scale field at $k \leq k_0$; see Fig. 9. This is found by calculating the spectrum of the magnetic field from simulations with 256^3 meshpoints and a domain size of $L_x = L_y = L_z = 8\pi/k_0$. In other words, a dynamo is observed but it is *not* a large-scale dynamo. This is corroborated by the TFM which produces positive turbulent diffusivity and vanishing α in all the aforementioned cases. In case (a) $\eta_t = +0.135 u_0/k_0$ for $A = 1$ and $B = 0$, and $\eta_t = +0.146 u_0/k_0$ for $A = 1$ and $B = 1$; in case (b) $\eta_t = +0.158 u_0/k_0$. However, in case (c) the TFM becomes unstable.

In conclusion, the magnetic field structure of dynamos from the modified TG flows is quite different from that of dynamos from the Roberts-IV flow. In the latter, the mean fields contributed about 50 per cent to the total field; see Fig. 2, while for the former, most of the power occurred at small scales. No significant mean magnetic field could thus be identified.

5 CONCLUSIONS

In this work, we have revisited the Roberts-IV flow using the TFM to compute the full set of turbulent transport coefficients. We confirm an earlier result of Tilgner (2004) that a dynamo is possible and that all components of the α tensor are vanishing. In addition, we confirm the result of Roberts (1972) that there is a finite horizontally averaged mean magnetic field, which should be explicable in terms of mean-field dynamo theory. The TFM reveals that the turbulent diffusivity tensor is isotropic in the horizontal plane. Moreover, in the regime where the dynamo is excited, the turbulent diffusivity is sufficiently strongly negative such that the eddy (molecular plus turbulent) diffusivity is negative. This is an unusual situation in that the horizontal components of the mean field are completely decoupled and grow independently with arbitrary relative amplitudes and phase shifts, but the same growth rate.

Many laminar flows are only slow dynamos, i.e. the growth rate goes to zero for large R_m . The Roberts-IV flow is no exception. These dynamos are therefore not expected to be astrophysically relevant. However, the method used to analyse such dynamos (TFM combined with DNS) is now playing an important role in the study of astrophysical dynamos for turbulent flows. This work highlights the accuracy of this method in that it enables us to pinpoint the detailed nature of a dynamo exhibiting a finite averaged magnetic field.

In the present case of laminar flow patterns, non-locality is crucially important. In other words, turbulent transport is described by a convolution of suitable integral kernels with the mean fields in space and time rather than just a multiplication. The TFM is particularly well suited to deal with such cases. For generic turbulent flows, as shown in earlier works by Hubbard & Brandenburg (2009) and Rheinhardt & Brandenburg (2012), we expect these transport kernels to have a relatively simple form and that complicated kernels, such as found here and in the earlier work (Rädler & Brandenburg 2009) are atypical. Note, however, that even though most astrophysical flows are turbulent and are expected to become statistically homogeneous and isotropic at small scales; in practice, large-scale anisotropy and inhomogeneity play an important role. In many of those cases, non-locality cannot be neglected and many Fourier modes need to be taken into account, as demonstrated by Chatterjee et al. (2011) for flows driven by the magnetic buoyancy instability.

ACKNOWLEDGEMENTS

We thank Alessandra Lanotte for inspiring us to look for negative eddy diffusivity dynamos, and Matthias Rheinhardt, Karl-Heinz Rädler and the referee for detailed comments regarding our paper. Financial support from the Scientific & Technological Research Council of Turkey (TÜBİTAK) and the European Research Council under the AstroDyn Research Project 227952 are gratefully acknowledged. The computations have been carried out at the National Supercomputer Centre in Umeå and at the Center for Parallel Computers at the Royal Institute of Technology in Sweden.

REFERENCES

- Brandenburg A., 2005, *Astron. Nachr.*, 326, 787
- Brandenburg A., Subramanian K., 2005, *Phys. Rep.*, 417, 1
- Brandenburg A., Rädler K.-H., Rheinhardt M., Käpylä P. J., 2008a, *ApJ*, 676, 740
- Brandenburg A., Rädler K.-H., Schirmer M., 2008b, *A&A*, 482, 739
- Brandenburg A., Svedin A., Vasil G. M., 2009, *MNRAS*, 395, 1599

- Chatterjee P., Mitra D., Rheinhardt M., Brandenburg A., 2011, *A&A*, 534, A46
- Hubbard A., Brandenburg A., 2009, *ApJ*, 706, 712
- Hubbard A., Del Sordo F., Käpylä P. J., Brandenburg A., 2009, *MNRAS*, 398, 1891
- Krause F., Rädler K.-H., 1980, *Mean-Field Magnetohydrodynamics and Dynamo Theory*. Pergamon Press, Oxford
- Lanotte A., Noullez A., Vergassola M., Wirth A., 1999, *Geophys. Astrophys. Fluid Dyn.*, 91, 131
- Mitra D., Brandenburg A., 2012, *MNRAS*, 420, 2170
- Rädler K.-H., 1976, in Bumba V., Kleczek J., eds, *Proc. IAU Symp. No. 71, Basic Mechanisms of Solar Activity*. Reidel, Dordrecht, p. 323
- Rädler K.-H., Brandenburg A., 2009, *MNRAS*, 393, 113
- Rädler K.-H., Brandenburg A., Del Sordo F., Rheinhardt M., 2011, *Phys. Rev. E*, 84, 4
- Rheinhardt M., Brandenburg A., 2010, *A&A*, 520, A28
- Rheinhardt M., Brandenburg A., 2012, *Astron. Nachr.*, 333, 71
- Roberts G. O., 1972, *Phil. Trans. R. Soc. A*, 271, 411
- Schrinner M., Rädler K.-H., Schmitt D., Rheinhardt M., Christensen U., 2005, *Astron. Nachr.*, 326, 245
- Schrinner M., Rädler K.-H., Schmitt D., Rheinhardt M., Christensen U. R., 2007, *Geophys. Astrophys. Fluid Dyn.*, 101, 81
- Steenbeck M., Krause F., Rädler K.-H., 1966, *Z. Naturforsch.*, 21a, 369; see also the translation in Roberts & Stix, *The turbulent dynamo*, Tech. Note 60, NCAR, Boulder, Colorado (1971)
- Sur S., Brandenburg A., Subramanian K., 2008, *MNRAS*, 385, L15
- Tilgner A., 2004, *Geophys. Astrophys. Fluid Dyn.*, 98, 225
- Zheligovsky V. A., 2011, *Springer Lecture Notes in Physics*, Vol. 829, *Large-Scale Perturbations of Magnetohydrodynamic Regimes*. Springer, Berlin
- Zheligovsky V. A., Podvigina O. M., Frisch U., 2001, *Geophys. Astrophys. Fluid Dyn.*, 95, 227

This paper has been typeset from a $\text{\TeX}/\text{\LaTeX}$ file prepared by the author.